

Rowan University

Rowan Digital Works

School of Osteopathic Medicine Faculty
Scholarship

School of Osteopathic Medicine

4-7-2020

Histidine-Triad Hydrolases Provide Resistance to Peptide-Nucleotide Antibiotics.

Eldar Yagmurov

Skolkovo Institute of Science and Technology

Darya Tsibulskaya

Skolkovo Institute of Science and Technology

Alexey Livenskiy

Russian Academy of Sciences

Marina Serebryakova

Russian Academy of Sciences

Yury I Wolf

NCBI, National Library of Medicine

See next page for additional authors

Follow this and additional works at: https://rdw.rowan.edu/som_facpub



Part of the [Bacteriology Commons](#), [Cell Biology Commons](#), [Immunoprophylaxis and Therapy Commons](#), [Medicine and Health Sciences Commons](#), and the [Pathogenic Microbiology Commons](#)

Recommended Citation

Yagmurov E, Tsibulskaya D, Livenskiy A, Serebryakova M, Wolf YI, Borukhov S, Severinov K, Dubiley S. Histidine-triad hydrolases provide resistance to peptide-nucleotide antibiotics. *mBio*. 2020 Apr 7;11(2). pii: e00497-20. doi: 10.1128/mBio.00497-20. PMID: 32265328. PMCID: PMC7157772.


This Article is brought to you for free and open access by the School of Osteopathic Medicine at Rowan Digital Works. It has been accepted for inclusion in School of Osteopathic Medicine Faculty Scholarship by an authorized administrator of Rowan Digital Works.

Authors

Eldar Yagmurov, Darya Tsibulskaya, Alexey Livenskiy, Marina Serebryakova, Yury I Wolf, Sergei Borukhov, Konstantin Severinov, and Svetlana Dubiley



Histidine-Triad Hydrolases Provide Resistance to Peptide-Nucleotide Antibiotics

Eldar Yagmurov,^a Darya Tsubluskaya,^{a,b} Alexey Livenskiy,^{b,c} Marina Serebryakova,^{b,d}  Yury I. Wolf,^e Sergei Borukhov,^f Konstantin Severinov,^{a,g,h} Svetlana Dubiley^{a,b}

^aCenter for Life Sciences, Skolkovo Institute of Science and Technology, Skolkovo, Russia

^bInstitute of Gene Biology, Russian Academy of Science, Moscow, Russia

^cFaculty of Bioengineering and Bioinformatics, Lomonosov Moscow State University, Moscow, Russia

^dA.N. Belozersky Institute of Physico-Chemical Biology, Lomonosov Moscow State University, Moscow, Russia

^eNational Center for Biotechnology Information, National Library of Medicine, Bethesda, Maryland, USA

^fDepartment of Cell Biology and Neuroscience, Rowan University School of Osteopathic Medicine, Stratford, New Jersey, USA

^gCenter for Precision Genome Editing and Genetic Technologies for Biomedicine, Institute of Gene Biology, Russian Academy of Sciences, Moscow, Russia

^hWaksman Institute for Microbiology, Piscataway, New Jersey, USA

ABSTRACT The *Escherichia coli* microcin C (McC) and related compounds are potent Trojan horse peptide-nucleotide antibiotics. The peptide part facilitates transport into sensitive cells. Inside the cell, the peptide part is degraded by nonspecific peptidases releasing an aspartamide-adenylate containing a phosphoramidate bond. This nonhydrolyzable compound inhibits aspartyl-tRNA synthetase. In addition to the efficient export of McC outside the producing cells, special mechanisms have evolved to avoid self-toxicity caused by the degradation of the peptide part inside the producers. Here, we report that histidine-triad (HIT) hydrolases encoded in biosynthetic clusters of some McC homologs or by stand-alone genes confer resistance to McC-like compounds by hydrolyzing the phosphoramidate bond in toxic aspartamide-adenosine, rendering them inactive.

IMPORTANCE Uncovering the mechanisms of resistance is a required step for countering the looming antibiotic resistance crisis. In this communication, we show how universally conserved histidine-triad hydrolases provide resistance to microcin C, a potent inhibitor of bacterial protein synthesis.

KEYWORDS HinT, RiPPs, antibiotics, histidine-triad proteins, microcin C, peptide-nucleotides

Microcin C (McC) is a ribosomally synthesized posttranslationally modified peptide (RiPP) antibiotic produced by some strains of *Escherichia coli*. Homologous compounds are encoded by gene clusters in numerous Gram-negative and Gram-positive bacteria (1). McC is produced by *E. coli* cells harboring a conjugative plasmid containing the *mccABCDE* cluster (2). The *mccA* gene encodes a seven-amino-acid precursor peptide whose C-terminal residue is modified by the product of the *mccB* gene to yield a peptidyl-adenylate McC¹¹²⁰, in which the C-terminal aspartamide is linked to AMP through a nonhydrolyzable *N*-acyl phosphoramidate linkage (Fig. 1) (3). McC¹¹²⁰ is further modified by MccD and the N-terminal domain of MccE protein, whose joint action results in a fully matured microcin C, McC¹¹⁷⁷, harboring an aminopropyl decoration on the phosphate moiety (Fig. 1) (4). Both forms of McC are exported from the producing cell by a specialized transporter encoded by the *mccC* gene (5).

McC acts through a Trojan horse mechanism. The peptide part facilitates uptake into the susceptible cell; once inside the cell, the peptide part is proteolytically degraded by aminopeptidases, releasing toxic “processed McC,” a nonhydrolyzable aspartamide-

Citation Yagmurov E, Tsubluskaya D, Livenskiy A, Serebryakova M, Wolf YI, Borukhov S, Severinov K, Dubiley S. 2020. Histidine-triad hydrolases provide resistance to peptide-nucleotide antibiotics. *mBio* 11:e00497-20. <https://doi.org/10.1128/mBio.00497-20>.

Editor Susan Gottesman, National Cancer Institute

Copyright © 2020 Yagmurov et al. This is an open-access article distributed under the terms of the [Creative Commons Attribution 4.0 International license](https://creativecommons.org/licenses/by/4.0/).

Address correspondence to Konstantin Severinov, severik@waksman.rutgers.edu, or Svetlana Dubiley, svetlana.dubiley@gmail.com.

This article is a direct contribution from Konstantin V. Severinov, a Fellow of the American Academy of Microbiology, who arranged for and secured reviews by Michael Ibba, The Ohio State University; Sylvie Rebuffat, CNRS, Muséum National d'Histoire Naturelle; and Konstantinos Beis, Imperial College London.

Received 3 March 2020

Accepted 11 March 2020

Published 7 April 2020

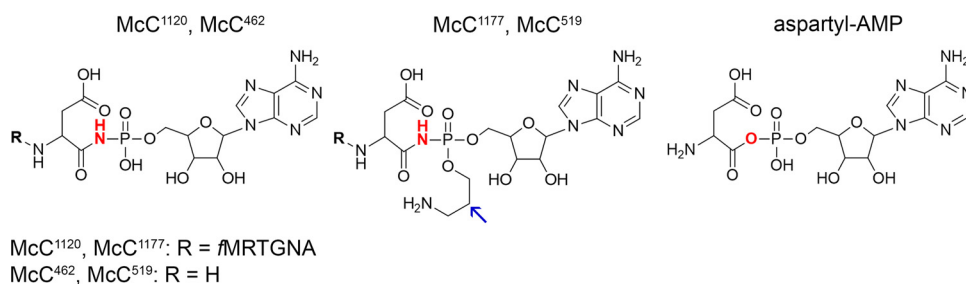


FIG 1 Structures of nonaminopropylated (McC¹¹²⁰) and aminopropylated (McC¹¹⁷⁷) *E. coli* microcin C, processed forms (McC⁴⁶² and McC⁵¹⁹, respectively), and Asp-AMP, an intermediate of AspRS-catalyzed reaction. The amino-propyl group is indicated by an arrow.

adenylate (Fig. 1), a structural mimic of intermediate of the reaction of aminoacylation of tRNA^{Asp} catalyzed by aspartyl-tRNA synthetase (AspRS) (6, 7). Processed McC competitively inhibits AspRS, bringing protein biosynthesis to a halt (5).

Although most McC is efficiently exported outside the producing cell by the MccC pump, intracellular processing by aminopeptidases should inevitably lead to the accumulation of toxic nonhydrolyzable aspartamide-adenylate and self-intoxication of the producer, since MccC does not export processed McC. Many *mcc*-like clusters acquired additional genes whose products help avoid self-intoxication. In the case of *E. coli*, the C-terminal domain of MccE, a Gcn5-related *N*-acetyltransferase (GNAT)-type acetyltransferase, acetylates the α -amino group of processed McC, making it unable to bind to AspRS (8). In addition, MccF peptidase cleaves the carboxamide bond between the C-terminal aspartamide and AMP of both intact and processed McC (9).

In this work, we report a novel pathway of McC inactivation by histidine-triad (HIT) superfamily hydrolases encoded in some *mcc*-like biosynthetic clusters or by stand-alone genes located elsewhere in bacterial genomes. Proteins of the HIT superfamily form two separate functional groups: the first group includes nucleotide hydrolases, represented by HinT (10–13), Fhit (13), APTX (14), and Dcsp (15) enzymes, while the other group includes nucleotide transferases such as GalT (16). The most common members of the HIT superfamily, HinT proteins, were shown to possess phosphoramidase activity (17). We show that bacterial MccH, a product of a gene in an *mcc*-like cluster from *Hyalangium minutum*, as well as its homologs from *Salmonella enterica*, *Nocardia kunsanensis*, and *Pseudomonas fluorescens*, are phosphoramidasases that confer resistance to McC-like compounds by hydrolyzing the toxic aspartamide-adenylate that is produced after intracellular processing of peptidyl-nucleotides.

RESULTS

Bioinformatic prediction and experimental validation of an unusual *mcc* operon of *Hyalangium minutum*. Bioinformatics analysis reveals a uniquely organized cluster in the genome of the Gram-negative bacterium *Hyalangium minutum* DSM 14724 that may determine the production of two putative McC-like compounds. The cluster contains two genes coding for putative precursor peptides, MccA₁ and MccA₂, two *mccB* genes, encoding THIF-like adenylyl transferases, and three genes whose products likely constitute a complex ABC-type transporter with integrated HlyD-like translocator and C39-like peptidase (18) (Fig. 2A). An additional gene, *mccH*, is located downstream of the *mccB*₁ gene and encodes a protein belonging to a histidine-triad (HIT) superfamily (12).

To validate the predicted *H. minutum* *mcc*-like cluster, *in vitro* adenylation reactions of synthetic MccA₁ and MccA₂ peptides with recombinant MccB₁ and MccB₂ adenylyl-transferases were performed and products analyzed by matrix-assisted laser desorption ionization–time of flight mass spectrometry (MALDI-TOF MS). As can be seen from Fig. 2B and C, incubation of the 36-amino-acid-long MccA₁ (MH⁺ at *m/z* 3,926.2) but not the 46-amino-acid-long MccA₂ (MH⁺ at *m/z* 4,767.6) with MccB₁ and an equimolar mixture of four nucleotide triphosphates led to the appearance of a mass ion at *m/z*

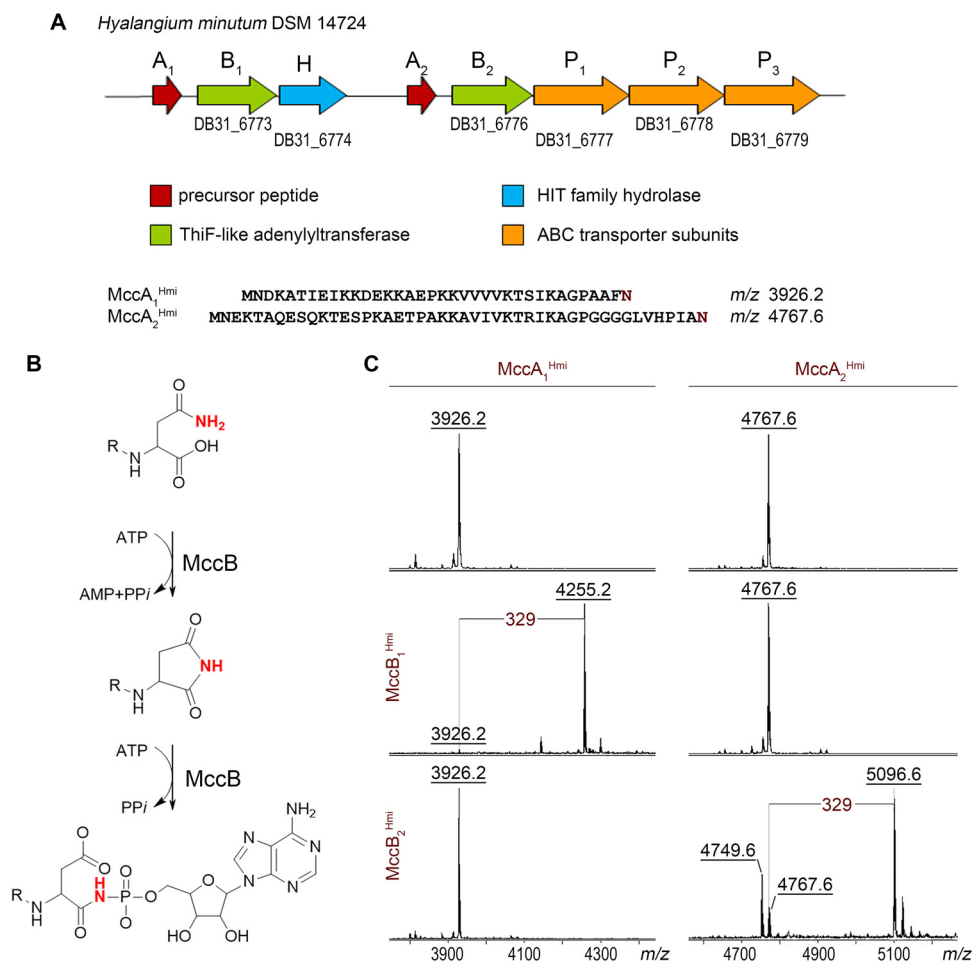


FIG 2 The *mcc*-like operon of *H. minutum* DSM 14724 and its products. (A) Organization of the *mcc*-like gene cluster from *H. minutum* DSM 14724. Genes are represented by colored arrows, with functional predictions corresponding to each color shown in the key beneath. (B) The mechanism of MccB-mediated adenylation of an MccA precursor peptide (3). (C) MALDI-TOF MS spectra of products of *in vitro* reactions between chemically synthesized *H. minutum* MccA₁ and MccA₂ precursor peptides and recombinant MccB₁^{Hmi} and MccB₂^{Hmi} enzymes in the presence of ATP. Spectra shown at the top are controls (no MccB enzyme added). The mass difference of 329 Da between MccA₁ (*m/z* 3,926.2) and MccA₂ (*m/z* 4,767.6) mass ions and the mass ions of the reaction products (*m/z* 4,255.2 and *m/z* 5,096.6, correspondingly) matches the modification with AMP; the MH⁺ ion at *m/z* 4,749.6 present in reaction mixtures containing MccA₂^{Hmi} and MccB₂^{Hmi} is a succinimide intermediate of the nucleotidyl transfer reaction.

4,255.2. The 329-Da mass increase corresponds to the adenylated form of the peptide. Conversely, in the presence of MccB₂, a prominent MH⁺ ion at *m/z* 5,096.6 was observed in reaction mixtures containing MccA₂, corresponding to its adenylated form. An MH⁺ ion at *m/z* 4,749.6 with 18 mass units less than the original MccA₂ ion was also detected. It corresponds to an MccB-catalyzed adenylation reaction intermediate, a succinimide derivative of the MccA₂ peptide. MccA₁ was not modified by MccB₂. We conclude that the *H. minutum* *mcc*-like cluster directs the synthesis of two peptidyl-adenylates, each synthesized from separate precursors by dedicated MccB enzymes.

We next attempted to reconstruct the production of each of the *H. minutum* Mcc-like compounds in a heterologous *E. coli* host. Cognate *mccA*-*mccB* pairs were cloned on one expression plasmid, and the *mccP*₁*P*₂*P*₃ genes encoding the putative transporter were cloned on a compatible plasmid. Under conditions of induction of plasmid-borne genes, *E. coli* cells or cellular extracts harboring both plasmid pairs did not inhibit the growth of an Mcc-sensitive *E. coli* tester strain, and no mass ions corresponding to *H. minutum* Mcc-like compounds were detected in cultured medium (see Fig. S1A in the supplemental material). To test if peptidyl-adenylates are synthe-

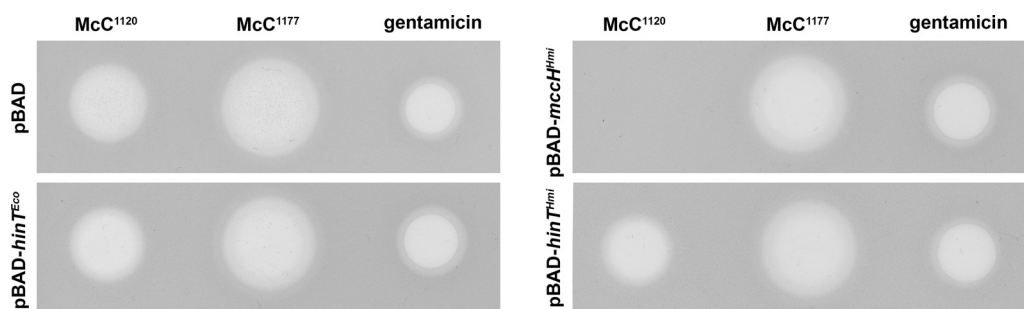


FIG 3 Overproduction of MccH^{Hmi} makes *E. coli* resistant to McC¹¹²⁰ but not to mature *E. coli* microcin C McC¹¹⁷⁷. Three microliters of 5 μ M solutions of McC¹¹⁷⁷, McC¹¹²⁰, or 0.5 μ g/ml gentamicin used as a control was deposited on lawns of *E. coli* cells harboring indicated plasmids. The results of overnight growth at 37°C under conditions of the induction of plasmid-borne genes are shown.

sized but fail to export from the heterologous host, induced cells were subjected to MALDI-TOF MS. MH⁺ ions at m/z 4,255.2 and 5,096.6 corresponding to full-length adenylated MccA₁ and MccA₂, respectively, were identified in cells harboring plasmids producing MccA₁-MccB₁ and MccA₂-MccB₂ pairs. In addition, MH⁺ ions at m/z 4,124.2 and 4,965.6, corresponding to adenylated MccA₁ and MccA₂ peptides lacking the first methionine residue, were detected. Unmodified full-sized MccA₁ and MccA₂ polypeptides (MH⁺ ions at m/z 3,926.2 and 4,767.6, respectively) and their derivatives lacking methionine (MH⁺ ions at m/z 3,795.2 and 4,636.6) were also observed (Fig. S1B). Thus, two distinct products of the *H. minutum* mcc cluster are produced in the heterologous host but fail to be exported at a detectable level.

MccH^{Hmi} confers McC immunity when overproduced in *E. coli*. We hypothesized that MccH^{Hmi} is a HIT superfamily phosphoramidase that provides *H. minutum* with self-immunity through the inactivation of McC-like compounds. To check this conjecture, we cloned the *mccH^{Hmi}* gene in an arabinose-inducible *E. coli* expression vector. We also created plasmids overproducing HinT^{Hmi}, a product of a standalone *H. minutum* gene, and its *E. coli* homologue HinT^{Eco}. Since the final toxic aspartate-adenylate forms of McC produced by *H. minutum* and *E. coli* should be identical (Fig. 1, McC⁴⁶²), we tested the susceptibility of MccH- or HinT-expressing cells to *E. coli* McC¹¹²⁰. Additionally, we used the aminopropylated form of *E. coli* McC, McC¹¹⁷⁷. In the assay, the drops of solutions of two active forms of *E. coli* McC were deposited on lawns of *E. coli* B McC-sensitive cells producing HIT proteins or harboring control empty vector (Fig. 3). The results revealed that the size of the growth inhibition zones around drops of fully mature McC¹¹⁷⁷ solution on lawns of HIT protein-producing cells was the same as that on the control cell lawn. In contrast, *E. coli* cells overexpressing the *mccH^{Hmi}* gene were completely resistant to McC¹¹²⁰, an intermediate of the *E. coli* McC maturation process that does not contain the aminopropyl moiety. The expression of either *hinT^{Eco}* or *hinT^{Hmi}* had no effect on the size of growth inhibition zones produced by McC¹¹²⁰ (Fig. 3). All HIT proteins were produced in comparable amounts, as judged by SDS-PAGE (Fig. S2). We therefore conclude that the MccH^{Hmi} but not HinT proteins tested can provide resistance to externally added toxic peptidyl-adenylate.

MccH^{Hmi} hydrolyzes the phosphoramidate bond connecting the aminoacyl and nucleotide moieties of processed McC¹¹²⁰. To determine the mechanism of MccH^{Hmi}-mediated resistance to toxic peptidyl-nucleotide, recombinant MccH^{Hmi}, HinT^{Hmi}, and HinT^{Eco} were purified and incubated with unprocessed McC¹¹²⁰ or McC¹¹⁷⁷, and the reaction products were analyzed by reverse-phase high-performance liquid chromatography (RP-HPLC) and MALDI-TOF MS. No changes were observed after a 1-h incubation (data not shown). Since no hydrolytic activity against either form of *E. coli* McC was detected, we considered whether the processed forms of McC¹¹²⁰ and McC¹¹⁷⁷ could be the substrates of MccH^{Hmi}. To this end, aspartamide-adenylates with (McC⁵¹⁹) and without (McC⁴⁶²) the aminopropyl group were prepared by *in vitro* processing of McC¹¹⁷⁷ and McC¹¹²⁰ (see Materials and Methods). After incubation with

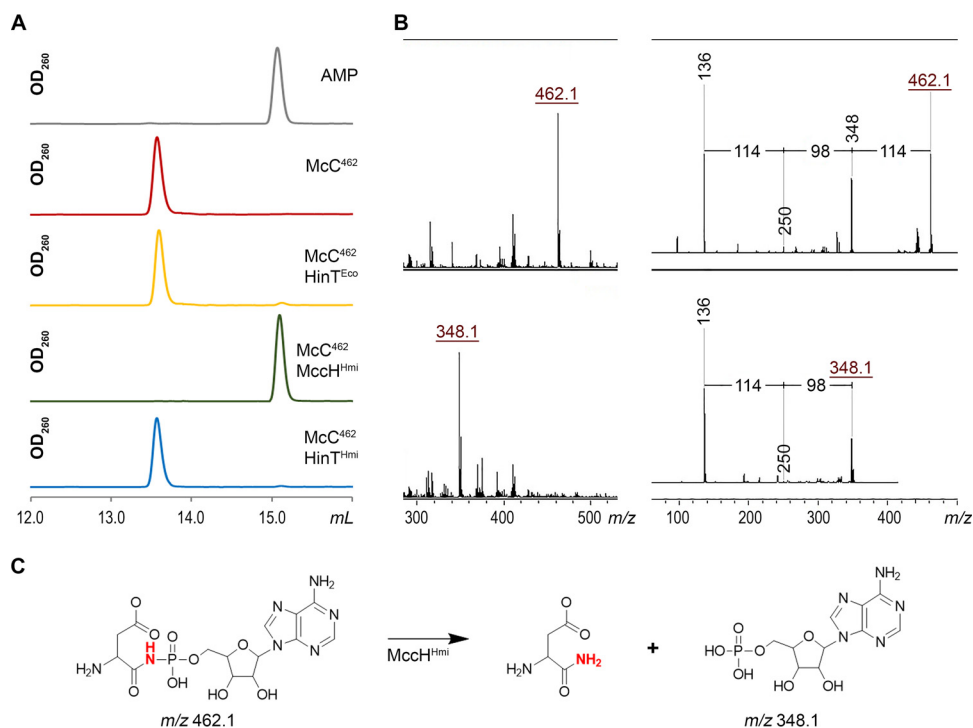


FIG 4 McCH^{Hmi} hydrolyzes aspartamide-adenylate McC⁴⁶². (A) RP HPLC elution profiles of the products of incubation of aspartamide-adenylate McC⁴⁶² with McCH^{Hmi}, HinT^{Hmi}, and HinT^{Eco}. (B) MALDI-TOF MS and MS-MS fragmentation analyses of McC⁴⁶² and the product of its hydrolysis by McCH^{Hmi}. For a description of the mass ions, refer to the text. (C) Scheme of an aspartamide-adenylate hydrolysis reaction by McCH^{Hmi}.

McCH^{Hmi}, HinT^{Hmi}, or HinT^{Eco}, samples were analyzed by RP-HPLC and MALDI-TOF MS. Since the expected phosphoramidase activity of McCH^{Hmi} should result in the appearance of AMP or adenosine 5'-phosphoramidate, we used AMP as a marker (Fig. 4A). Upon a 1-h incubation with McCH^{Hmi}, McC⁴⁶² was completely converted into a new compound with the same chromatographic mobility as AMP (Fig. 4A). The MH⁺ ion of this compound had *m/z* 348.1, matching that of AMP (Fig. 4B). The MS-MS fragmentation spectra confirmed this assignment (Fig. 4B). None of the enzymes was able to hydrolyze fully processed microcin with aminopropyl decoration (McC⁵¹⁹) (Fig. S3).

In the presence of HinT^{Eco} or HinT^{Hmi}, McC⁴⁶² remained largely intact, with only trace amounts of AMP formed in the course of the reaction. We therefore decided to assess whether HinT^{Hmi} is an active phosphoramidase using AMP-*N*-ε-(*N*-α-acetyl-lysine methyl ester)-5'-phosphoramidate (εK-AMP), a previously described HinT phosphoramidase model substrate (17). Incubation of εK-AMP with HinT^{Hmi}, HinT^{Eco}, or McCH^{Hmi}, followed by RP-HPLC and MALDI-TOF MS, revealed that both HinT^{Hmi} and HinT^{Eco} hydrolyzed it with the release of AMP, while McCH^{Hmi} did not (Fig. 5A to C). We therefore conclude that the McCH^{Hmi} hydrolase cleaves the P-N bond in aspartamide-adenylate but not in εK-AMP. HinT^{Hmi} and HinT^{Eco} have different specificities, where they hydrolyze εK-AMP well but are largely inactive toward processed McC¹¹²⁰ (Fig. 4A and 5A). These results explain why both HinT enzymes failed to provide resistance to McC in the antibiotic susceptibility test under our conditions *in vivo* (Fig. 3).

McCH homologs are present in diverse bacteria. HIT domain-containing proteins are widespread among prokaryotes (see Materials and Methods for details on domain identification). A phylogenetic tree constructed using available HIT domain sequences revealed that McCH^{Hmi} belongs to a distinct clade, highlighted in red in Fig. 6A (see also Fig. S4). This clade also contains proteins from putative *mcc*-like clusters from *Nocardiosis*, *Pseudomonas*, and *Thermobifida* spp., as well as multiple proteins encoded by standalone genes. Genes encoding McCH homologs from the *mcc*-like cluster from *Nocardiosis kunsanensis* DSM 44524, as well as standalone genes from *Pseudomonas*

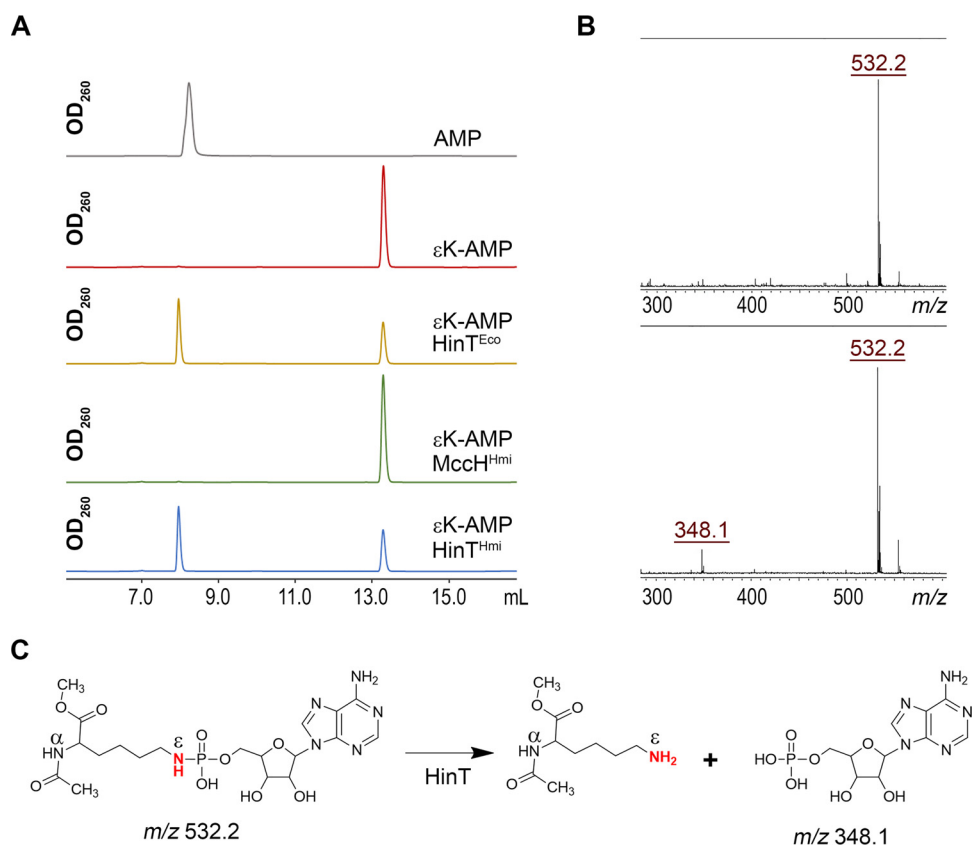


FIG 5 Substrate specificity of MccH^{Hmi}, HinT^{Hmi}, and HinT^{Eco} phosphoramidases. (A) HPLC elution profiles of products of incubation of εK-AMP with HinT^{Eco}, HinT^{Hmi}, or MccH^{Hmi}. (B) MALDI-TOF MS analysis of the hydrolysis reaction of the εK-AMP by HinT^{Hmi} protein. (C) Scheme of a HinT-mediated hydrolysis reaction of εK-AMP (36).

fluorescens A506, *Salmonella enterica* serovar Newport, *Microcystis aeruginosa* PCC9809, and *Parcubacteria* sp. strains GWA24037 and DG742, were cloned into an *E. coli* expression vector, and the ability of the resulting plasmids to make *E. coli* cells resistant to the two forms of McC was tested. As can be seen from Fig. 6B, overexpression of most MccH-like genes led to resistance to McC¹¹²⁰ but not to McC¹¹⁷⁷. The apparently inactive MccH-like proteins from *M. aeruginosa* strain PCC9809 and *Parcubacteria* sp. strain DG742 are the earliest branching MccH homologs tested, and they may have evolved different substrate specificities.

Mutational analysis of MccH active center. The mechanism of nucleotide phosphoramidate hydrolysis is best studied for the *E. coli* enzyme, HinT^{Eco} (19), and its human homologue, hHint1 (20, 21). The characteristic feature of the HIT superfamily proteins is a conserved histidine-triad motif, HxHxHxx, where H is a histidine, and x is a hydrophobic residue (12). The three essential catalytic histidines form a network of hydrogen bonds with the substrate that promotes proton transfer from the protonated C-terminal histidine of the triad (H103 in HinT^{Eco} or H102 in HinT^{Hmi}) to phosphoramidate unbridged oxygens and amide nitrogen and facilitate nucleophilic attack of the central histidine (HinT^{Eco} H101 or HinT^{Hmi} H100) on the phosphorus atom, resulting in P-N bond hydrolysis (19, 21, 22). Another conserved His residue, H39 in HinT^{Eco} (H38 in HinT^{Hmi}), located outside the triad motif closer to the N terminus of HIT enzymes, contributes to catalysis by stimulating the protonation of the third histidine of the triad by stabilizing its cationic state (21). Mutational analysis of human Hint1, a close homologue of HinT^{Eco}, revealed that substitutions of conserved histidines equivalent to H39 and H103 in HinT^{Eco} substantially reduce the catalytic activity (22).

Interestingly, HIT proteins of the MccH clade contain a modified motif where the third histidine is substituted for lysine (K103 in MccH^{Hmi}). Together with this substit-

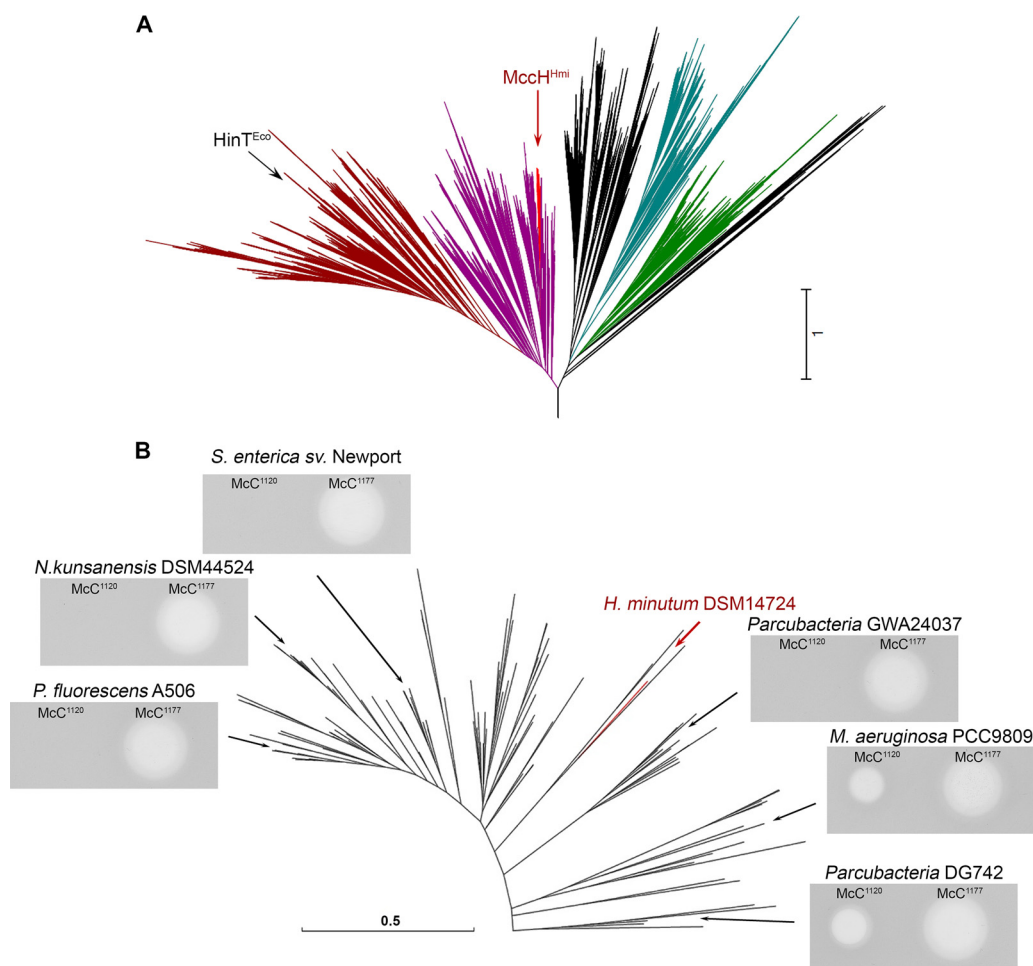


FIG 6 Diversity of McC-specific phosphoramidases. (A) Approximate maximum likelihood (ML) phylogenetic tree of the HIT domain proteins from completely sequenced genomes. Dark magenta and dark red indicate HinT-like proteins (dark red shows the protein kinase C interacting protein-related subgroup), bright red indicates the MccH^{Hmi} clade that is expanded in panel B, cyan indicates GalT, and green indicates FHIT. In black are clades without any clear profile signature. The arrows point to HinT^{Eco} (within the PKCI clade) and MccH^{Hmi}. (B) Approximate ML phylogenetic tree of proteins within the MccH^{Hmi} clade and growth inhibition zones formed by McC¹¹²⁰ and McC¹¹⁷⁷ on lawns of *E. coli* B cells transformed with plasmids expressing MccH^{Hmi} or homologs from the indicated positions on the tree. The MccH^{Hmi} branch is highlighted in red. sv., serovar.

tion, MccH-like proteins lost the N-terminal conserved histidine (H39 in HinT^{Eco}), which is replaced by phenylalanine (F44 in MccH^{Hmi}) (Fig. 7A and S4). Structural modeling (see below) indicates that F44 makes hydrophobic contacts with the side chain of K103 in MccH^{Hmi} (Fig. 8A). In addition, all members of MccH clade acquired glutamate (E93 in MccH^{Hmi}) five residues away from the triad motif. In the structural model of MccH^{Hmi}, E93 makes a hydrogen bond (or a salt bridge) with K103, thus playing the same functional role as H39 in HinT^{Eco} (H38 in HinT^{Hmi}) (Fig. 8). Since this triple substitution should still allow phosphoramidate bond hydrolysis, we speculate that the positively charged lysine occupying position of H103 in MccH^{Hmi} ultimately donates its stationary proton to the nitrogen of the phosphoramidate bond (Fig. 8B). To test this conjecture and better understand the origin of MccH-like protein specificity, we prepared two MccH^{Hmi} mutants harboring the single substitutions K103H and F44H. An MccH^{Hmi} K103H-F44H double mutant was also engineered. As a key residue in the triad, H101 in MccH^{Hmi} is supposed to directly participate in catalysis. Therefore, a protein with substitution H101N was prepared and tested for phosphoramidase activity. As expected, the H101N mutant, which served as a control, was catalytically inactive, i.e., no hydrolysis of processed McC¹¹²⁰ was detected (Fig. 7B). The K103H substitution had also eliminated

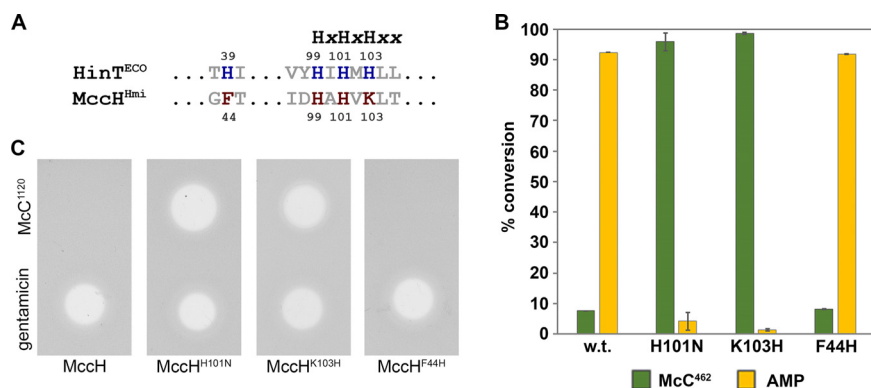


FIG 7 Mutational analysis of active site residues of McCH^{Hmi}. (A) Sequence alignment of the conserved HIT motif of HinT^{Eco} and McCH^{Hmi}. (B) Phosphoramidase activity of McCH^{Hmi} active-site mutants. *In vitro* reaction mixtures containing aspartamide-adenylate McC⁴⁶² were incubated with wild-type McCH^{Hmi} and the mutant proteins, containing the H101N or K103N substitution, and then analyzed by RP-HPLC. The conversion of McC⁴⁶² was calculated as the percentage of McC⁴⁶² and AMP absorption peak areas that remained after the reaction completion relative to the corresponding peak areas observed without the addition of enzymes. The bars represent the mean \pm standard deviation (SD) conversion percentages calculated from three independent measurements. (C) Mutations in the active center of McCH^{Hmi} abolish immunity to McC¹²⁰. Growth inhibition of *E. coli* cells harboring pBAD plasmids encoding the indicated proteins. Solutions (5 μ M) of McC¹²⁰ and 0.5 μ g/ml gentamicin were deposited on freshly prepared lawns and allowed to grow overnight at 37°C under conditions of induction of plasmid-borne genes.

the hydrolytic activity of McCH^{Hmi}, confirming that a lysine characteristic of McCH-like proteins is essential for the catalytic function. The F44H mutant retained its activity, which is also an expected result. The K103H-F44H double mutant was insoluble, and thus, its enzymatic properties could not be assessed. To confirm the *in vitro* hydrolytic activity of the mutants, the *E. coli* cells harboring the corresponding plasmids were tested for their susceptibility to McC¹²⁰. As shown in Fig. 7C, the H101N and K103H substitutions completely abolished immunity to peptidyl-adenylates, while the phenotype of McCH^{Hmi} F44H-expressing cells was indistinguishable from that of the cells producing wild-type McCH^{Hmi}.

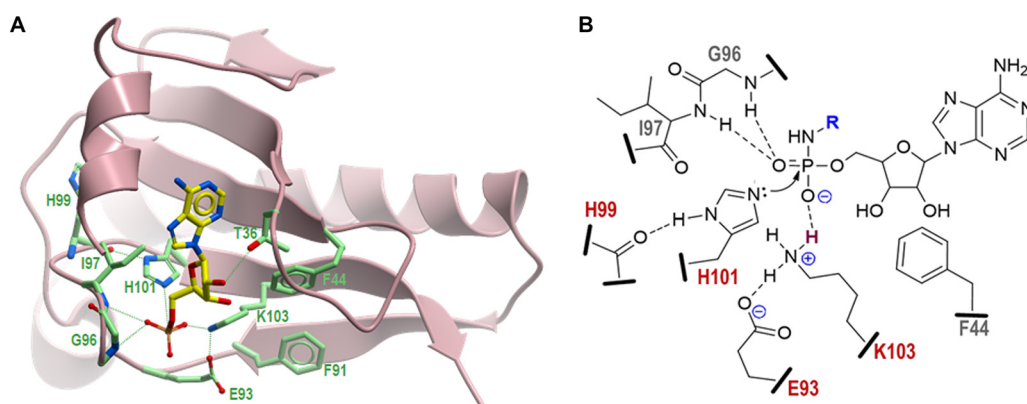


FIG 8 Three-dimensional structural model of McCH^{Hmi} and proposed catalytic mechanism. (A) Model structure of McCH^{Hmi} generated by the SWISS-MODEL homology modeling server (23) using as the template the crystal structures of the HIT-like protein from *Mycobacterium paratuberculosis* (PDB 3POT) (24) and human HINT1-AMP complex (PDB 3TW2) (28). Positions of catalytic residues in the McCH^{Hmi} active site in complex with AMP are shown as atom type-colored sticks: N, blue; O, red; P, orange. The C atoms in AMP are in yellow, and the C atoms in the side chains are in light green. (B) Schematic diagram representing the active site of McCH^{Hmi} with the bound substrate, aspartamide-adenylate (the aspartyl moiety is represented by R and shown in blue). Residues of the ExxxxHxHxKxx motif conserved among all members of the McCH clade that are directly involved in the catalysis are shown in red. Potential hydrogen bonds between peptide side chains, backbone atoms, and phosphate oxygens are indicated by dashed lines. The proton to be transferred from the ϵ -amino group of K103 to the unbridged oxygen of the phosphoramidate is depicted in dark red. Nucleophilic attack of the unprotonated nitrogen of H101 on electrophilic phosphorus atom is shown by a curved arrow.

Structural model of MccH^{Hmi}. The loss of functional activity by MccH^{Hmi} mutant K103H suggested that this residue, which is specific to MccH clade proteins, is involved in substrate binding and/or catalysis. We also hypothesized that some other active-site residues might spatially constrain the catalytic pocket environment favoring the flexible aliphatic side chain of lysine over a more rigid imidazole ring of histidine. To explore the possible spatial organization of the active center of MccH^{Hmi}, we generated its three-dimensional (3D) model using the SWISS-MODEL homology modeling program (23). The resulting model of MccH^{Hmi} (Fig. 8A) is based on a top-ranked *Mycobacterium paratuberculosis* HIT-like protein structure (PDB 3P0T) (24) with a global model quality estimate (GMQE) quality score of 0.68, indicative of good reliability and accuracy. To reveal the potential interactions in the substrate-binding pocket, the model structure of MccH^{Hmi} was superimposed with the crystal structure of the human histidine-triad nucleotide-binding protein 1 (hHINT1) in complex with AMP (PDB 3TW2) (25).

As expected, the overall structure of MccH^{Hmi} and the spatial organization of its active site are very similar to those of other HinT and HIT-like proteins, with a notable exception of the C-terminal nonconserved 45 amino acids that model differently depending on the homology template used. In the model, MccH^{Hmi} forms a symmetric homodimer with each protein monomer capable of binding and hydrolyzing the substrate (Fig. S5). The nucleoside-binding pocket is formed mostly by conserved hydrophobic residues F11, F12, L15, F34, P37, V46, F38, and I97. The hydroxyl group of T36 makes a hydrogen bond with ribose 2'-OH in AMP, thus contributing to nucleotide recognition. The N atoms of the side chains of catalytic H101 and K103 are positioned (2.5 to 2.7 Å) to make strong hydrogen bonds with the P and unbridged O atoms of the phosphate moiety of AMP, respectively (Fig. 8A). The interatomic distances (2.9 to 3.6 Å) between the peptide backbone amide and carbonyl groups of residues G96, I97, and H99 and their interacting partners (unbridged oxygen and the protonated N atom of H101, respectively) are within a range that is optimal for hydrogen bonding and consistent with the proposed catalytic mechanism (Fig. 8B). Unexpectedly, the carbonyl group of E93, a conserved residue among members of the MccH clade, is in close proximity (2.3 Å) to the protonated N atom of K103, suggesting a strong hydrogen bond or salt bridge that would stabilize the charged state of K103 and facilitate the catalysis. Furthermore, consistent with the results of our mutagenesis experiments (Fig. 7), the bulky hydrophobic side chains of F44 and F91 replacing conserved H39 and I86 in HinT^{Eco} and HinT^{Hmi}, about the side chain of K103, stabilize its conformation and direct it toward the phosphate. Thus, the positioning of F44, F91, and E93 in the active center explains the observed preference for a catalytic lysine in MccH instead of histidine in the HinT clade.

DISCUSSION

In this work, we uncover a novel mechanism of immunity to microcin C-like compounds by MccH^{Hmi}, a HIT-like phosphoramidase encoded in the *mcc* cluster of *H. minutum*. The cluster produces two separate peptide-adenylates that are analogous to McC¹¹²⁰, a toxic maturation intermediate of *E. coli* McC that lacks the aminopropyl decoration. As of today, the *mcc* operon from *H. minutum* is the only validated operon that produces two McC-like compounds with different peptide parts. Since peptide parts determine the specificity of antibacterial action by allowing selective import into sensitive cells (26), *H. minutum* DSM 14724 may target distinct, nonoverlapping sets of its competitors by the McC-like compounds it produces.

Like other McC-producing organisms, *H. minutum* should experience the buildup of toxic processed products inside the cell, which could lead to the cessation of protein biosynthesis. The MccH^{Hmi} enzyme, the product of the *mcc* operon, alleviates this problem by cleaving the bond between phosphorus and nitrogen in the toxic aspartamide-adenylate that is produced after proteolytic processing of either of the two McC-like compounds encoded by the operon, thus providing self-immunity to the producing cell. MccH^{Hmi} makes cells resistant to the maturation intermediate of *E. coli* McC that lacks the aminopropyl decoration but not to fully mature McC¹¹⁷⁷. The

catalytic mechanism of phosphoramidate hydrolysis requires a transient protonation of two unbridged oxygens (21, 22). The presence of an additional aminopropyl group on the phosphate in unprocessed MccC¹¹⁷⁷ and processed MccC⁵¹⁹ precludes the proton transfer reaction and renders the phosphorus center inaccessible to nucleophilic attack by the catalytic histidine (HinT^{Eco} H101, HinT^{Hmi} H100, or MccH^{Hmi} H101). Thus, *H. minutum* and *E. coli* *mcc* operons use different strategies to overcome the self-intoxication of producers. The *H. minutum* *mcc* operon produces two peptidyl-adenylates without additional modifications, and the processing of both compounds leads to identical toxic aspartamide-adenylate. MccH^{Hmi} hydrolyzes the phosphoramidate bond in aspartamide-adenylate with the formation of AMP and aspartamide. The absence of additional genes in the *H. minutum* *mcc* operon that may be involved in self-immunity suggests that MccH^{Hmi} is sufficient to counter the inhibitory effects caused by the buildup of the toxic product. In *E. coli*, the MccD/E enzyme complex installs the aminopropyl decoration at the phosphate of peptide-adenylate, which allows the potency of antibacterial action to be increased ~10-fold by increasing the affinity of the processed compound to its target, AspRS (4). The presence of activity-enhancing decoration renders the MccH^{Hmi} enzyme inactive, necessitating another mechanism to overcome self-intoxication. MccE detoxifies both aminopropylated and nonaminopropylated aspartamide-adenylates by acetylating the amino group of the aspartate (8).

The structural model of MccH^{Hmi} built based on a crystal structure of homologous HIT-like protein from *M. paratuberculosis* (PDB 3POT) (24) provides a plausible view on a spatial organization of the active center and offers clues to understanding the enzyme's substrate specificity. Importantly, the model points to the functional role of the conserved hydrophobic (F44 and F91) and charged (E93) residues in the activation of catalytic K103 for the hydrolysis of aspartamide-adenylate that can be tested experimentally. It is also predicted that residues M95 and W115 of the C-terminal loop of one MccH monomer together with L110 from the adjacent C-terminal loop of the other MccH monomer form a tight aspartamide-binding site which would sterically occlude the binding of bulkier groups, such as the ϵ -lysine amide of ϵ K-AMP. This view is consistent with the fact that HinT^{Eco} lacking the C-terminal extension present in MccH^{Hmi} was active toward ϵ K-AMP but could not hydrolyze aspartamide-adenylate. It is also supported by previous observations that both deletion and swapping of the C-terminal loop between human HINT1 and HinT^{Eco} strongly affect both the catalytic activity and substrate specificity (19, 27, 28). The proposed model will be validated in our future genetic, biochemical, and structural studies of bacterial MccH and HinT proteins.

Previous studies have shown that bacterial and human HinT proteins exhibit a broad substrate specificity; they can accommodate both purine and pyrimidine nucleotides with various substitutions in the aminoacyl moiety, including D- and L-stereoisomers of tryptophan and sterically hindering *N*- ϵ -(*N*- α -acetyl-lysine methyl ester)-adenosine phosphoramidates (11, 27). Unlike HinT, the MccH^{Hmi} and its homologues from four diverse bacterial species characterized in this work apparently have evolved much more specialized enzymes that show a clear preference for aspartamide-adenylate (Fig. 4 and 5). Our results suggest that the fully processed Mcc is a bona fide substrate for MccH. We speculate that MccH-like proteins from *M. aeruginosa* PCC9809 and *Parcubacteria* sp. DG742, which are inactive toward *E. coli* Mcc, may recognize yet-unidentified species-specific Mcc-like compounds that carry different nucleoside or amino acid moieties.

MATERIALS AND METHODS

Molecular cloning. *E. coli* DH5 α was used for cloning. All primers were synthesized by Evrogen (Russia); their sequences are listed in Table S1. The *H. minutum* DSM 14724 or *E. coli* BW25113 genomic DNA was used as the template for PCR. Phusion DNA polymerase (Thermo Scientific) was used for PCR.

For MccB^{Hmi} and MccB₂^{Hmi} activity analysis, their coding sequences were amplified from the *H. minutum* DSM 14724 genomic DNA. The PCR products were digested with BamHI and Sall restriction endonucleases and inserted under the same sites into the pET22_MBP vector (26) to create an N-terminal fusion protein with a maltose-binding protein (MBP) tag.

For the heterologous *mcc^{Hmi}* expression system, a DNA fragment spanning the *mccP₁^{Hmi}*, *mccP₂^{Hmi}*, and *mccP₃^{Hmi}* genes was amplified from genomic DNA, digested with EcoRI and KpnI, and inserted into pACYCDuet-1 vector (Novagen-Millipore, USA) linearized with the same restriction endonucleases. To construct MccA-MccB expression vectors, first, the phosphorylated self-complementary oligonucleotides containing sequences of the *MccA₁^{Hmi}* and *MccA₂^{Hmi}* open reading frames (ORFs) were inserted into the pRSFDuet-1 vector (Novagen-Millipore, USA) and digested with NcoI and HindIII, resulting in the pRSF-MccA₁^{Hmi} and pRSF-MccA₂^{Hmi} vectors, respectively. Then, *mccB₁^{Hmi}* and *mccB₂^{Hmi}* were PCR amplified, digested with NdeI and KpnI, and inserted into the pRSF-*mccA₁^{Hmi}* and pRSF-*mccA₂^{Hmi}* vectors linearized with NdeI and KpnI, resulting in pRSF-*mccA₁B₁^{Hmi}* and pRSF-*mccA₂B₂^{Hmi}*, respectively.

To obtain an arabinose-inducible vector for the heterologous expression of HIT proteins, the pBAD/His B vector (Invitrogen-Thermo Fisher, USA) was linearized by PCR with the appropriate primers that contained an introduced ribosomal binding site and Sall and HindIII restriction sites to generate pBAD30_SalRBS. Next, the *mccH^{Hmi}*, *hinT^{Hmi}*, and *hinT^{Eco}* genes were PCR amplified using genomic DNA as the template and the corresponding primers. Genes encoding the homologs of MccH^{Hmi} were purchased as synthetic DNA fragments from IDT, USA. All amplified PCR products and synthetic fragments were digested with Sall and HindIII and inserted between the same sites into the pBAD30 expression vector.

To create vectors for HIT protein fused with C-terminal His₆ tags for protein purification, the *mccH^{Hmi}*, *hinT^{Hmi}*, and *hinT^{Eco}* genes were PCR amplified, digested with NdeI and XhoI, and inserted into the pET22(b) vector (Novagen-Millipore, USA). The site-directed mutagenesis of *mccH^{Hmi}* was carried out using overlap extension PCR (29), with appropriate primers.

Recombinant protein expression and purification. Recombinant proteins were produced in *E. coli* BL21(DE3) transformed with the appropriate plasmid. The cells were grown in 500 ml of TB medium supplemented with ampicillin to an optical density at 600 nm (OD₆₀₀) of ~0.7 and induced with 0.2 mM isopropyl-β-D-thiogalactopyranoside (IPTG). After induction, the culture was transferred for overnight growth at 18°C and 180 rpm. The cells were harvested by centrifugation at 8,000 × *g* and 4°C for 20 min, resuspended in ice-cold resuspension buffer (20 mM Tris-HCl, 300 mM NaCl, 1 mM dithiothreitol [DTT] [pH 8.0]), supplemented with 1 mM phenylmethylsulfonyl fluoride (PMSF), and disrupted by sonication. For the His-tagged proteins, imidazole was added up to 2 mM. The lysate was cleared by centrifugation at 30,000 × *g* and 4°C for 20 min. The cleared lysate was applied to a preequilibrated column with a tag-binding resin; depending on the tag present, either amylose resin (NEB) or Talon CellThru Co²⁺-chelating resin (TaKaRa-Clontech) was used. The resin was washed with 10 column volumes of resuspension buffer, followed by elution with 5 column volumes of the elution buffer (20 mM Tris-HCl [pH 8.0], 50 mM NaCl, 10% glycerol) supplemented with either 10 mM maltose or 0.5 M imidazole.

Adenylation of MccA₁^{Hmi} and MccA₂^{Hmi}. For validation of the MccA-MccB pairs of the *H. minutum* *mcc*-like gene cluster, *in vitro* modification of synthetic MccA₁^{Hmi} (MNDKATIEIKKDEKKAEPKVVVVKTSIK AGPAAFN) and MccA₂^{Hmi} (MNEKTAQESQKTESPKAETPAKKAVIVKTRIKAGPGGGGLVHPIAN) (GenScript, USA) peptides using purified MccB₁^{Hmi} and MccB₂^{Hmi} reactions was performed. Reaction mixtures contained 50 μM synthetic peptides (either MccA₁^{Hmi} or MccA₂^{Hmi}), 5 μM recombinant MccB₁^{Hmi} or MccB₂^{Hmi}, and 2 mM each nucleoside triphosphate (NTP) in the reaction buffer (50 mM Tris-HCl [pH 8.0], 150 mM NaCl, 10 mM MgCl₂, 5 mM DTT). The reaction was carried out at 30°C for 16 h and then stopped by the addition of 0.1% trifluoroacetic acid (TFA) in water. The products of the reaction were analyzed by MALDI-TOF MS for the presence of adenylation MccA₁^{Hmi} and MccA₂^{Hmi}.

Mcc₁^{Hmi} and Mcc₂^{Hmi} production test. *E. coli* BL21(DE3) cells harboring a combination of either pRSF-*mccA₁B₁^{Hmi}* and pACYC-*mccP₁P₂P₃^{Hmi}* or pRSF-*mccA₂B₂^{Hmi}* and pACYC-*mccP₁P₂P₃^{Hmi}* plasmids were grown in 25 ml of 2xYT medium (1.6% Tripton, 1% yeast extract, 0.5% NaCl) at 30°C with constant shaking at 180 rpm. Upon reaching an OD₂₆₀ of ~0.7, the cells were induced with 0.25 mM IPTG and grown for an additional 20 h at 30°C. After that, the cells were pelleted at 5,000 × *g* and resuspended in 250 μl of M9 medium. Aliquots of 15 μl were deposited on a freshly prepared M9 agar lawn of *E. coli* strain B harboring the pRSFDuet-1, pETduet-1, and pACYCDuet-1 vectors. Plates were incubated at 30°C overnight to allow formation of the lawn. The next day, the plates were inspected for the presence of growth inhibition zones. Additionally, the cells and the surrounding agar were analyzed for the presence of Mcc-like products using mass spectrometry.

In vivo immunity assay. *E. coli* strain B was transformed with pBAD_SalRBS vectors containing the *mccH^{Hmi}* gene or its homologues. The overnight cultures of the *E. coli* cells with the appropriate vectors were diluted 1,000-fold in M9 agar medium supplemented with 1% glycerol, 0.02% yeast extract, 10 mM arabinose, and 100 μg/ml ampicillin. The sensitivity of cells carrying plasmid-borne genes encoding HIT-like proteins was measured by applying 5-μl drops of 5 μM Mcc¹¹²⁰ and 5 μM Mcc¹¹⁷⁷ on the surface of the plate and allowed to dry, and gentamicin (0.5 μg/ml) was used as a control growth inhibitor. Plates were incubated for 16 h at 30°C for a lawn to form. The next day, the growth inhibition zones were analyzed.

εK-AMP synthesis. The synthesis of εK-AMP was performed as described elsewhere, with minor modifications (17). To synthesize εK-AMP, 0.12 g (6.25 mmol) of 1-ethyl-3-(3-dimethylaminopropyl) carbodiimide HCl (Sigma-Aldrich) was added to the flask containing 0.98 g (2.7 mmol) of AMP (Sigma-Aldrich), 0.1 g of (0.42 mmol) *N*-α-acetyl-L-lysine methyl ester HCl (Sigma-Aldrich), and 10 ml of ultrapure water, and the pH of the solution was adjusted with triethylamine to a value of 7.5. The mixture was incubated in the shaker at 65°C, with vigorous shaking at 250 rpm for 22 h. After allowing the reaction mix to cool down to room temperature, the mixture was lyophilized, redissolved in 0.1% TFA in water, and applied to a Luna 5-μm C₁₈ 100-Å, LC column (250 by 10 mm; Phenomenex). The purification of εK-AMP was performed in a linear gradient (5 to 25%) of acetonitrile. The fractions were analyzed for the

presence of ϵ K-AMP by MALDI-TOF mass spectrometry, and fractions containing ϵ K-AMP were subjected to additional chromatographic purification on the same column in a linear gradient of acetonitrile (0 to 25%) in triethylammonium acetate (TEAA) buffer (pH 6.5).

In vitro phosphoramidase activity assay. To test the phosphoramidase activity of McCH^{Hmi}, HinT^{Hmi}, HinT^{Eco} enzymes, and their respective variants, the processed forms of *E. coli* McC¹¹⁷⁷ and McC¹¹²⁰ (McC^{S19} and McC⁴⁶², respectively) and ϵ K-AMP were used as the substrates. For production, purification, and processing of McC forms, refer to the study by Metlitskaya et al. (6). Fifty micromolar processed McC or ϵ K-AMP was mixed with 5 μ M the enzyme in the reaction buffer (20 mM HEPES [pH 7.2], 2.5 mM MgCl₂, 2.5 mM MnCl₂). The reaction mixture was incubated at 25°C for 30 min, terminated by the addition of 0.1% TFA, and analyzed for hydrolysis by HPLC and mass spectrometry.

Reverse-phase HPLC analysis of the products of the in vitro reactions. All biochemical reactions were analyzed on 1220 Infinity II LC system (Agilent), and the peak separation occurred on a Zorbax Eclipse Plus C₁₈ 5- μ m (4.6 by 250 mm) column (Agilent) in a 0.1 M TEAA buffer system (pH 6.0) in the varying linear gradient of acetonitrile.

The products of McC⁴⁶² hydrolysis reactions were separated in a linear gradient of acetonitrile (0 to 20%) over a period of 15 min. After the incubation of McC^{S19} with HIT enzymes, the reaction products were separated in the acetonitrile gradient (0 to 22%) for 15 min. After hydrolysis of ϵ K-AMP by HIT enzymes, the reaction products were analyzed in the linear acetonitrile gradient (5 to 30%) lasting for 15 min. The chromatograms were processed with the use of the ChemStation software (Agilent), and elution profiles were exported in comma-separated values format.

Mass spectrometry analysis. One to two microliters of the sample aliquots was mixed with 0.5 μ l of matrix mix (Sigma-Aldrich) on a steel target. The mass spectra were recorded on an UltrafleXtreme MALDI-TOF/TOF mass spectrometer (Bruker Daltonics) equipped with a neodymium laser. The molecular MH⁺ ions were measured in reflector mode; the accuracy of the measured results was within 0.1 Da.

Sequence analysis. Proteins containing the histidine catalytic triad were identified in 4,621 completely sequenced genomes available in 2016. Profiles belonging to the NCBI CDD (30) superfamily cl00228 were used as PSI-BLAST (31) queries to search the protein sequences encoded in this set. The resulting set of 10,580 proteins was clustered using UCLUST (32) and aligned using MUSCLE (33) (Fig. S6); alignments were iteratively compared to each other using HHSEARCH and aligned using the HHALIGN program (34). The approximate ML tree was reconstructed using the FastTree program (35) with a WAG evolutionary model and gamma-distributed site rates.

SUPPLEMENTAL MATERIAL

Supplemental material is available online only.

FIG S1, PDF file, 0.2 MB.

FIG S2, PDF file, 0.1 MB.

FIG S3, PDF file, 0.1 MB.

FIG S4, PDF file, 0.4 MB.

FIG S5, PDF file, 0.1 MB.

FIG S6, PDF file, 0.3 MB.

TABLE S1, PDF file, 0.1 MB.

ACKNOWLEDGMENTS

This work was supported by NIH RO1 grant AI117270 (to K.S. and Satish A. Nair) and Skoltech institutional funds to K.S., Russian Science Foundation grants RSF 16-14-10356 and RSF 19-14-00266 to S.D., and Rowan University departmental funds to S.B. Y.I.W. is supported through the intramural program of the U.S. National Institutes of Health. Bioinformatic analysis was partially supported by the Ministry of Science and Higher Education of the Russian Federation grant 075-15-2019-1661.

The MALDI-TOF MS facility was made available to us as part of the framework of the Moscow State University Development Program PNG 5.13.

REFERENCES

- Severinov K, Semenova E, Kazakov A, Kazakov T, Gelfand MS. 2007. Low-molecular-weight post-translationally modified microcins. *Mol Microbiol* 65:1380–1394. <https://doi.org/10.1111/j.1365-2958.2007.05874.x>.
- Guijarro JI, González-Pastor JE, Baleux F, San Millán JL, Castilla MA, Rico M, Moreno F, Delepierre M. 1995. Chemical structure and translation inhibition studies of the antibiotic microcin C7. *J Biol Chem* 270:23520–23532. <https://doi.org/10.1074/jbc.270.40.23520>.
- Roush RF, Nolan EM, Löhr F, Walsh CT. 2008. Maturation of an *Escherichia coli* ribosomal peptide antibiotic by ATP-consuming N-P bond formation in microcin C7. *J Am Chem Soc* 130:3603–3609. <https://doi.org/10.1021/ja7101949>.
- Kulikovskiy A, Serebryakova M, Bantysh O, Metlitskaya A, Borukhov S, Severinov K, Dubiley S. 2014. The molecular mechanism of aminopropylation of peptide-nucleotide antibiotic microcin C. *J Am Chem Soc* 136:11168–11175. <https://doi.org/10.1021/ja505982c>.
- Severinov K, Nair SK. 2012. Microcin C: biosynthesis and mechanisms of bacterial resistance. *Future Microbiol* 7:281–289. <https://doi.org/10.2217/fmb.11.148>.
- Metlitskaya A, Kazakov T, Kommer A, Pavlova O, Praetorius-Ibba M, Ibba M, Krashennikov I, Kolb V, Khmel I, Severinov K. 2006. Aspartyl-tRNA synthetase is the target of peptide nucleotide antibiotic microcin C. *J Biol Chem* 281:18033–18042. <https://doi.org/10.1074/jbc.M513174200>.

7. Kazakov T, Vondenhoff GH, Datsenko KA, Novikova M, Metlitskaya A, Wanner BL, Severinov K. 2008. *Escherichia coli* peptidase A, B, or N can process translation inhibitor microcin C. *J Bacteriol* 190:2607–2610. <https://doi.org/10.1128/JB.01956-07>.
8. Novikova M, Kazakov T, Vondenhoff GH, Semenova E, Rozenski J, Metlytskaya A, Zukher I, Tikhonov A, Van Aerschot A, Severinov K. 2010. MccE provides resistance to protein synthesis inhibitor microcin C by acetylating the processed form of the antibiotic. *J Biol Chem* 285:12662–12669. <https://doi.org/10.1074/jbc.M109.080192>.
9. Tikhonov A, Kazakov T, Semenova E, Serebryakova M, Vondenhoff G, Van Aerschot A, Reader JS, Govorun VM, Severinov K. 2010. The mechanism of microcin C resistance provided by the MccF peptidase. *J Biol Chem* 285:37944–37952. <https://doi.org/10.1074/jbc.M110.179135>.
10. Krakowiak A, Pace HC, Blackburn GM, Adams M, Mekhalifa A, Kaczmarek R, Baraniak J, Stec WJ, Brenner C. 2004. Biochemical, crystallographic, and mutagenic characterization of hint, the AMP-lysine hydrolase, with novel substrates and inhibitors. *J Biol Chem* 279:18711–18716. <https://doi.org/10.1074/jbc.M314271200>.
11. Wang J, Fang P, Schimmel P, Guo M. 2012. Side chain independent recognition of aminoacyl adenylates by the Hint1 transcription suppressor. *J Phys Chem B* 116:6798–6805. <https://doi.org/10.1021/jp212457w>.
12. Brenner C. 2014. Histidine triad (HIT) superfamily. eLS. John Wiley & Sons Ltd., Chichester, United Kingdom. <https://doi.org/10.1002/9780470015902.a0020545.pub2>.
13. Brenner C. 2002. Hint, Fhit, and GalT: function, structure, evolution, and mechanism of three branches of the histidine triad superfamily of nucleotide hydrolases and transferases. *Biochemistry* 41:9003–9014. <https://doi.org/10.1021/bi025942q>.
14. Kijas AW, Harris JL, Harris JM, Lavin MF. 2006. Aprataxin forms a discrete branch in the HIT (histidine triad) superfamily of proteins with both DNA/RNA binding and nucleotide hydrolase activities. *J Biol Chem* 281:13939–13948. <https://doi.org/10.1074/jbc.M507946200>.
15. Liu H, Rodgers ND, Jiao X, Kiledjian M. 2002. The scavenger mRNA decapping enzyme Dcp5 is a member of the HIT family of pyrophosphatases. *EMBO J* 21:4699–4708. <https://doi.org/10.1093/emboj/cdf448>.
16. Holden HM, Rayment I, Thoden JB. 2003. Structure and function of enzymes of the Leloir pathway for galactose metabolism. *J Biol Chem* 278:43885–43888. <https://doi.org/10.1074/jbc.R300025200>.
17. Chou T-F, Bieganowski P, Shilinski K, Cheng JJ, Brenner C, Wagner CR. 2005. ³¹P NMR and genetic analysis establish hinT as the only *Escherichia coli* purine nucleoside phosphoramidase and as essential for growth under high salt conditions. *J Biol Chem* 280:15356–15361. <https://doi.org/10.1074/jbc.M500434200>.
18. Holland IB, Peherstorfer S, Kanonenberg K, Lenders M, Reimann S, Schmitt L. 13 December 2016, posting date. Type I protein secretion—deceptively simple yet with a wide range of mechanistic variability across the family. *EcoSal Plus* 2016 <https://doi.org/10.1128/ecosalplus.ESP-0019-2015>.
19. Bardaweel S, Pace J, Chou T-F, Cody V, Wagner CR. 2010. Probing the impact of the echinT C-terminal domain on structure and catalysis. *J Mol Biol* 404:627–638. <https://doi.org/10.1016/j.jmb.2010.09.066>.
20. Shah R, Maize KM, Zhou X, Finzel BC, Wagner CR. 2017. Caught before released: structural mapping of the reaction trajectory for the sofosbuvir activating enzyme, human histidine triad nucleotide binding protein 1 (hHint1). *Biochemistry* 56:3559–3570. <https://doi.org/10.1021/acs.biochem.7b00148>.
21. Liang G, Webster CE. 2017. Phosphoramidate hydrolysis catalyzed by human histidine triad nucleotide binding protein 1 (hHint1): a cluster-model DFT computational study. *Org Biomol Chem* 15:8661–8668. <https://doi.org/10.1039/c7ob02098h>.
22. Zhou X, Chou TF, Aubol BE, Park CJ, Wolfenden R, Adams J, Wagner CR. 2013. Kinetic mechanism of human histidine triad nucleotide binding protein 1. *Biochemistry* 52:3588–3600. <https://doi.org/10.1021/bi301616c>.
23. Waterhouse A, Bertoni M, Bienert S, Studer G, Tauriello G, Gumienny R, Heer FT, de Beer TAP, Rempfer C, Bordoli L, Lepore R, Schwede T. 2018. SWISS-MODEL: homology modelling of protein structures and complexes. *Nucleic Acids Res* 46:W296–W303. <https://doi.org/10.1093/nar/gky427>.
24. Baugh L, Phan I, Begley DW, Clifton MC, Armour B, Dranow DM, Taylor BM, Muruthi MM, Abendroth J, Fairman JW, Fox D, Dieterich SH, Staker BL, Gardberg AS, Choi R, Hewitt SN, Napuli AJ, Myers J, Barrett LK, Zhang Y, Ferrell M, Mundt E, Thompkins K, Tran N, Lyons-Abbott S, Abramov A, Sekar A, Serzhinskiy D, Lorimer D, Buchko GW, Stacy R, Stewart LJ, Edwards TE, Van Voorhis WC, Myler PJ. 2015. Increasing the structural coverage of tuberculosis drug targets. *Tuberculosis (Edinb)* 95:142–148. <https://doi.org/10.1016/j.tube.2014.12.003>.
25. Dolot R, Ozga M, Włodarczyk A, Krakowiak A, Nawrot B. 2012. A new crystal form of human histidine triad nucleotide-binding protein 1 (hHINT1) in complex with adenosine 5'-monophosphate at 1.38 Å resolution. *Acta Crystallogr Sect F Struct Biol Cryst Commun* 68:883–888. <https://doi.org/10.1107/S1744309112029491>.
26. Bantysh O, Serebryakova M, Zukher I, Kulikovskiy A, Tsibulskaya D, Dubiley S, Severinov K. 2015. Enzymatic synthesis and functional characterization of bioactive microcin C-like compounds with altered peptide sequence and length. *J Bacteriol* 197:3133–3141. <https://doi.org/10.1128/JB.00271-15>.
27. Chou T-F, Baraniak J, Kaczmarek R, Zhou X, Cheng J, Ghosh B, Wagner CR. 2007. Phosphoramidate pronucleotides: a comparison of the phosphoramidase substrate specificity of human and *Escherichia coli* histidine triad nucleotide binding proteins. *Mol Pharm* 4:208–217. <https://doi.org/10.1021/mp060070y>.
28. Chou T-F, Sham YY, Wagner CR. 2007. Impact of the C-terminal loop of histidine triad nucleotide binding protein1 (Hint1) on substrate specificity. *Biochemistry* 46:13074–13079. <https://doi.org/10.1021/bi701244h>.
29. Ho SN, Hunt HD, Horton RM, Pullen JK, Pease LR. 1989. Site-directed mutagenesis by overlap extension using the polymerase chain reaction. *Gene* 77:51–59. [https://doi.org/10.1016/0378-1119\(89\)90358-2](https://doi.org/10.1016/0378-1119(89)90358-2).
30. Marchler-Bauer A, Bo Y, Han L, He J, Lanczycki CJ, Lu S, Chitsaz F, Derbyshire MK, Geer RC, Gonzales NR, Gwadz M, Hurwitz DI, Lu F, Marchler GH, Song JS, Thanki N, Wang Z, Yamashita RA, Zhang D, Zheng C, Geer LY, Bryant SH. 2017. CDD/SPARCLE: functional classification of proteins via subfamily domain architectures. *Nucleic Acids Res* 45:D200–D203. <https://doi.org/10.1093/nar/gkw1129>.
31. Schaffer AA. 2001. Improving the accuracy of PSI-BLAST protein database searches with composition-based statistics and other refinements. *Nucleic Acids Res* 29:2994–3005. <https://doi.org/10.1093/nar/29.14.2994>.
32. Edgar RC. 2010. Search and clustering orders of magnitude faster than BLAST. *Bioinformatics* 26:2460–2461. <https://doi.org/10.1093/bioinformatics/btq461>.
33. Edgar RC. 2004. MUSCLE: a multiple sequence alignment method with reduced time and space complexity. *BMC Bioinformatics* 5:113–119. <https://doi.org/10.1186/1471-2105-5-113>.
34. Söding J. 2005. Protein homology detection by HMM-HMM comparison. *Bioinformatics* 21:951–960. <https://doi.org/10.1093/bioinformatics/bti125>.
35. Price MN, Dehal PS, Arkin AP. 2010. FastTree 2—approximately maximum-likelihood trees for large alignments. *PLoS One* 5:e9490. <https://doi.org/10.1371/journal.pone.0009490>.
36. Chou T-F, Wagner CR. 2007. Lysyl-tRNA synthetase-generated lysyl-adenylate is a substrate for histidine triad nucleotide-binding proteins. *J Biol Chem* 282:4719–4727. <https://doi.org/10.1074/jbc.M610530200>.
37. Zukher I, Pavlov M, Tsibulskaya D, Kulikovskiy A, Zybko T, Bikmetov D, Serebryakova M, Nair SK, Ehrenberg M, Dubiley S, Severinov K. 2019. Reiterative synthesis by the ribosome and recognition of the N-terminal formyl group by biosynthetic machinery contribute to evolutionary conservation of the length of antibiotic microcin C peptide precursor. *mBio* 10:e00768-19. <https://doi.org/10.1128/mBio.00768-19>.